Journal of the Brazilian Society of Mechanical Sciences and Engineering (2020) 42:624
https://doi.org/10.1007/s40430-020-02708-5

TECHNICAL PAPER

Global performance criterion of robotic manipulator with clearances based on reliability

Fabian Andres Lara-Molina[1] · **Didier Dumur**[2]

Received: 9 July 2020 / Accepted: 28 October 2020 / Published online: 13 November 2020

Abstract
This paper presents a novel performance criterion applied to robotic manipulators based on kinematic reliability. The kinetostatic performance criteria have been used to quantify the effect of errors in the manipulators. Nevertheless, design criteria based on the kinematic errors produced by joint clearances have not been established. This contribution proposes a novel performance index based on kinematic reliability concepts that evaluates the effect of the kinematic error produced by clearances over a required workspace. The application of the proposed global kinematic reliability criterion is evaluated for serial and parallel manipulators.

Keywords Robotic manipulators · Performance criteria · Error · Clearances · Kinematics · Reliability

1 Introduction

The design criteria are measures of mechanical properties that quantify the performance of robotic manipulators. Several design criteria have been established to quantify the capabilities of the manipulator by examining the dynamic and kinematic models. The kinematic criteria are based on the Jacobian matrix, and they quantify the kinematic behavior considering the kinetostatic performance [1]. The dynamic criteria evaluate the dynamic properties such as the inertia and the behavior of the elastic elements (elastic joints or links) regarding the elastodynamics [2]. Moreover, the workspace and singularities are widely used as criteria of manipulators [3]. The design criteria are classified as local and global criteria: local criteria evaluate the performance at a specific pose; on the other hand, global criteria examine the performance over the workspace of the manipulator. These design criteria are widely applied in the optimal mechanical design of robotic manipulators [4–6], and their definition is challenging due to the uncertainty involved in the specific task that the robot should execute [7].

The robotic manipulators are unavoidably affected by uncertainties produced by manufacturing and assembly error of the links, positioning error of the actuators and clearances of joints. In order to deal with the uncertainty in the geometric parameters, the calibration of the manipulator reduces significantly the effect of manufacturing and assembly errors of the links; nevertheless, the errors produced by joint clearances cannot be correctly compensated by the calibration procedures [8]. Moreover, advanced motion control techniques have been widely applied to minimize the positioning errors of the actuators [9, 10]. Nevertheless, the joint clearances are necessary for the relative motion between the links; therefore, the joint clearances are the most important source that introduces error and affects the accuracy and repeatability [11].

Consequently, the effect of the joint clearances should be taken into account in the design criteria of the robotic manipulator. In order to develop a novel design criterion that takes into account the kinematic positioning error is necessary to model the joint clearances produced by uncertainties and to compute kinematic positioning error of the manipulator produced by clearances. Zhu et al. [12] illustrate the uncertain behavior of joint clearances and its effects on the error of manipulators. The error prediction methods aim

Technical Editor: Adriano Almeida Gonçalves Siqueira.

✉ Fabian Andres Lara-Molina
fabianmolina@utfpr.edu.br

Didier Dumur
Didier.Dumur@centralesupelec.fr

[1] Federal University of Technology - Paraná, Cornélio Procópio, PR 86300-00, Brazil

[2] CentraleSupélec, Laboratoire des signaux et systèmes, Université Paris-Saclay, CNRS, 91190 Gif sur Yvette, France

at computing the error produced by the joint clearances on the end effector.

Initially, the clearances of rotational joints were modeled by using the bearing model that consists of a radial gap between the inner and outer rings of the joint [13, 14]. The model of the joint clearances has been used for several applications and analyses such as kinematic sensitivity analysis [15], error prediction analysis [16], dynamic analysis [14, 17], uncertainty analysis [12, 18], and workspace analysis [19]. Regarding the error prediction methods, several approaches have been developed to assess the influence of joint clearances on the kinematic accuracy of the manipulator [15, 16, 20].

The kinematic reliability of manipulators determines the probability of obtaining positioning errors within acceptable limits. The kinematic reliability has recently emerged as alternative criteria to evaluate the effects of uncertainties in manipulators [21]. Kim et al [22] evaluated the kinematic reliability of manipulators using the advanced first-order second moment (AFOSM) method. Pandey and Zhang [23] used the fractional moments to efficiently compute the kinematic reliability such that the positioning error remains within acceptable limits. Cui et al. [24] computed the kinematic reliability using the Monte Carlo simulation method, and they evaluated three error sensitivity criteria based on the singular value decomposition of the error translation matrix. Zhan et al. [25] proposed an hybrid method based on the first-order second moment to evaluate the uncertainties of a planar parallel manipulator modeled as random and interval variables. Xu [21] studied the influence of each error source on the kinematic reliability of a delta parallel manipulator. Zhang and Han [26] developed an efficient reliability analysis method to account for random dimensions and joint angles of robotic mechanisms. Moreover, further developments about the kinematic reliability have recently been reported in literature considering improvements in the computational methods [27–29], application on industrial robots [30, 31], and applications on planar mechanisms [32]. The research works mentioned above evaluated the reliability as a local property, i.e., the kinematic reliability was assessed at a specific pose of the manipulator. Nevertheless, it is necessary to compute the kinematic reliability as a global criteria.

The kinetostatic performance criteria have been used to quantify the effect of errors in the manipulators [33]. Nevertheless, design criteria based on errors produced by joint clearances have not been established. This contribution proposes a novel performance index based on kinematic reliability concepts that evaluates the effect of the error produced by clearances over a required workspace. The contribution of the present research effort is composed of three stages: *i*) the introduction of random uncertainties within the axisymmetric model of the clearances, *ii*) the formulation of an error propagation method for the uncertain clearances, and *iii*) the global reliability criterion.

This paper is organized into four sections: Initially, the axisymmetric model of joint clearances with uncertainties and the error propagation method is presented. Then, the global kinematic reliability criterion is defined. Afterward, the proposed global kinematic criterion is applied to serial and parallel manipulators through numerical simulations. Finally, the conclusion and further work are presented.

2 Clearances and error propagation method

2.1 Joint clearance model

The axisymmetric model of the joint clearance is inspired from the model showed by Meng at al. [16] and Binaud at al. [15]. The further developments or our contribution consist in introducing uncertainties within the parameters that define the clearances.

Clearances introduce additional and uncontrollable degrees of freedom within the joints according to the axisymmetric joint clearance model that considers the joint axis along the z-axis (see Fig. 1). These additional degrees of freedom can be either rotational or translational; consequently, the pose error at the local frame $F_{i,j}$ of the joint can be modeled using the error screw $\delta\mathbf{e}_{i,j}$, thus:

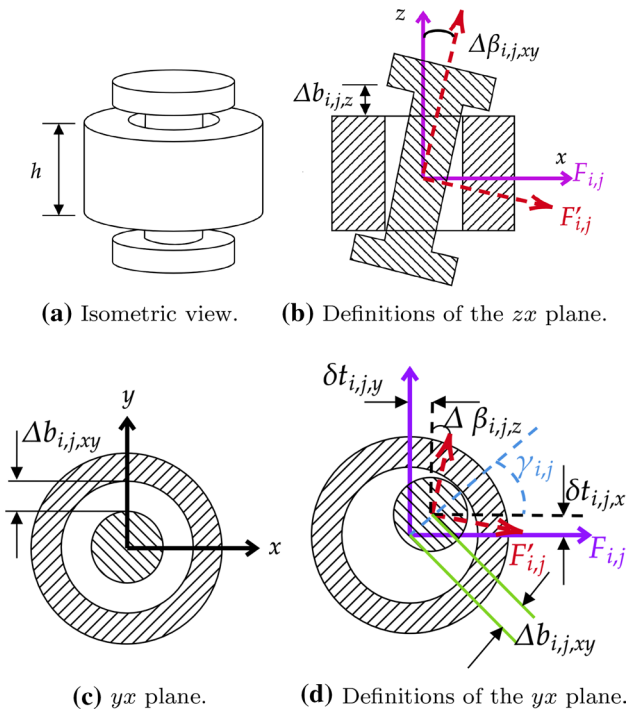

(a) Isometric view. **(b)** Definitions of the zx plane.

(c) yx plane. **(d)** Definitions of the yx plane.

Fig. 1 Joint clearance model

$$\delta\mathbf{e}_{i,j} = \left[\delta\mathbf{r}_{i,j}\ \ \delta\mathbf{t}_{i,j}\right]^T \tag{1}$$

where i is the index of the kinematic chain, and j is the index of the joint in the respective i^{th} kinematic chain, $\delta\mathbf{r}_{i,j} = \left[\delta r_{i,j,x}\ \delta r_{i,j,y}\ \delta r_{i,j,z}\right]^T$ is the orientation error, and $\delta\mathbf{t}_{i,j} = \left[\delta t_{i,j,x}\ \delta t_{i,j,y}\ \delta t_{i,j,z}\right]^T$ is the translational error produced by the clearances of the auxiliary frame $F'_{i,j}$ with respect to the local frame $F_{i,j}$ (see Fig. 1).

The translational clearance along the axis joint z and the rotational clearance with respect to the axis z are defined as $\Delta b_{i,j,z}$ and $\Delta\beta_{i,j,xy}$, respectively. Moreover, the translational clearance in the xy plane and the rotational clearance related to the z axis are defined as $\Delta b_{i,j,xy}$ and $\Delta\beta_{i,j,z}$. Therefore, the elements of the error screw $\delta\mathbf{e}_{i,j}$ of Eq. (1) are defined in Eq. (2).

$$\begin{cases} \delta r_{i,j,x} = \Delta\beta_{i,j,xy}\cos(\gamma_{i,j}) \\ \delta r_{i,j,y} = \Delta\beta_{i,j,xy}\sin(\gamma_{i,j}) \\ \delta r_{i,j,z} = \Delta\beta_{i,j,z} \end{cases} \quad \begin{cases} \delta t_{i,j,x} = \Delta b_{i,j,xy}\cos(\gamma_{i,j}) \\ \delta t_{i,j,x} = \Delta b_{i,j,xy}\sin(\gamma_{i,j}) \\ \delta t_{i,j,z} = \Delta b_{i,j,z} \end{cases} \tag{2}$$

with $0 \leq \gamma_{i,j} \leq 2\pi$. Following this definition, the positioning and orientation error should meet the following constraints: $\delta r^2_{i,j,x} + \delta r^2_{i,j,y} \leq \Delta\beta^2_{i,j,xy}$ and $\delta t^2_{i,j,x} + \delta t^2_{i,j,y} \leq \Delta b^2_{i,j,xy}$. The uncertainties are introduced in the following five parameters that define the clearances of the joints: $\Delta\beta_{i,j,z}$, $\Delta\beta_{i,j,xy}$, $\gamma_{i,j}$, $\Delta b_{i,j,xy}$ and $\Delta b_{i,j,z}$. These uncertainties are modeled as random variables according to the expression presented in Eq. (3).

$$\begin{aligned} \Delta\beta_{i,j,z}(\Omega) &= \beta_z + \beta_z\xi(\Omega) \\ \Delta\beta_{i,j,xy}(\Omega) &= \beta_{xy} + \beta_{xy}\xi(\Omega) \\ \gamma_{i,j}(\Omega) &= \gamma + \gamma\xi(\Omega) \\ \Delta b_{i,j,xy}(\Omega) &= b_{xy} + b_{xy}\xi(\Omega) \\ \Delta b_{i,j,z}(\Omega) &= b_z + b_z\xi(\Omega) \end{aligned} \tag{3}$$

with β_z, β_{xy}, γ, b_{xy}, and b_z being the mean values of each uncertain parameter, $\xi(\Omega)$ is a Gaussian random variable, and Ω represents a random process.

The vector of the set of uncertain clearance parameters from a serial kinematic chain is defined based on Eq. (3) as:

$$\mathbf{c} = \left[\mathbf{c}_1\ \mathbf{c}_2\ \ldots\ \mathbf{c}_i\ \ldots\ \mathbf{c}_{n_{i,f}}\right] \tag{4}$$

where $i = 1, \ldots, n_i$, and $n_{i,f}$ represents the number of joints of the kinematic chain; $\mathbf{c}_j$ are the uncertain parameters of the $j-th$ joint clearance, and thus, $\mathbf{c}_j = \left[\Delta\beta_{j,z}(\Omega)\ \Delta\beta_{j,xy}(\Omega)\ \gamma_j(\Omega)\ \Delta b_{j,xy}(\Omega)\ \Delta b_{j,z}(\Omega)\right]$.

2.2 Error propagation method

The error propagation method of serial manipulators is based on the method proposed by Binaud at al. [15]. Nevertheless, further developments and improvements have been included in the present contribution for parallel manipulators.

2.2.1 Serial kinematic chain

Initially, the Denavit–Hartenberg method is used to obtain the pose of the end effector considering no clearances. Thus, the homogeneous transformation matrix, $\mathbf{S}_{i,j}$, is defined as:

$$\mathbf{S}_{i,j} = \begin{bmatrix} \mathbf{R}_{i,j} & \mathbf{t}_{i,j} \\ \mathbf{0}_{1\times3} & 1 \end{bmatrix} \tag{5}$$

where $i = 1, \ldots, m$ and $j = 1, \ldots, n_{i,f}$, respectively; m is the number of kinematic chains (for a single kinematic chain $m = 1$), and $n_{i,f}$ is the total number of frames. $\mathbf{S}_{i,j}$ represents the transformation matrix from the frame $\mathbf{F}_{i,j}$ to the frame $\mathbf{F}_{i,j+1}$, $\mathbf{R}_{i,j}$ is the (3x3) rotation matrix, and $\mathbf{t}_{i,j}$ is the (3x1) position vector. The pose of the end effector related to the $i-th$ kinematic chain, $\mathbf{P}_i$, is defined as:

$$\mathbf{P}_i = \prod_{j=1}^{n_{i,f}} \mathbf{S}_{i,j} \tag{6}$$

However, the pose of the end effector considering the joint clearances, $\mathbf{P}'_i$, will not be equal to the pose $\mathbf{P}_i$ presented in Eq. (6). The adjoint map transformation matrix of $\mathbf{S}_{i,j}$ maps the error screw onto the end effector at a specific pose as presented in Eq. (7).

$$adj(\mathbf{S}_{i,j}) = \begin{bmatrix} \mathbf{R}_{i,j} & \mathbf{0}_{3\times3} \\ \mathbf{T}_{i,j}\mathbf{R}_{i,j} & \mathbf{R}_{i,j} \end{bmatrix} \tag{7}$$

where $\mathbf{T}_{i,j}$ is the screw matrix of the vector $\mathbf{t}_{i,j}$; $\mathbf{t}_{i,j}$ and $\mathbf{R}_{i,j}$ can be extracted from the transformation matrix of Eq. (5). Moreover, the adjoint of the inverse transformation matrix, $adj(\mathbf{S}_{i,j})^{-1}$, permits to express screws at the frame $\mathbf{F}_{i,j+1}$ from $\mathbf{F}_{i,j}$.

The error screw, $\delta\mathbf{e}_{i,j}$, in the local frame $\mathbf{F}_{i,j}$, can be expressed in the end-effector frame, $\mathbf{F}_{i,n_{i,f}}$, by multiplying all the inverse adjoint transformation matrices from $n_{i,f}$ to $j+1$, and thus, $\left(\prod_{k=n_{i,f}}^{j+1} adj(\mathbf{S}_{i,k})^{-1}\right)\delta\mathbf{e}_{i,j}$.

The following expression quantifies the pose error of the end effector considering all the joint clearances:

$$\delta\mathbf{p}_i|\mathbf{F}_{i,P} = \sum_{j=1}^{n_i}\prod_{k=n_{i,f}}^{j+1} adj(\mathbf{S}_{i,k})^{-1}\delta\mathbf{e}_{i,j} \tag{8}$$

where n_i being the number of joints, and $n_{i,f}$ the number of frames; note that $n_{i,f} \geq n_i$. $\delta_{\mathbf{p}_i}|\mathbf{F}_{i,P}$ is the pose error in the frame attached to the end effector $\mathbf{F}_{i,P}$.

The pose error in the end effector should be expressed in the reference frame attached to the fixed base $F_{i,1}$. Thus,

$$\delta\mathbf{p}_i|\mathbf{F}_{i,1} = \prod_{j=1}^{n_{i,f}} \left(\mathbf{N}_{i,j}\right)\delta\mathbf{p}_i|F_{i,P} \tag{9}$$

where $\mathbf{N}_{i,j} = \begin{bmatrix} \mathbf{R}_{i,j} & \mathbf{0}_{3\times3} \\ \mathbf{0}_{3\times3} & \mathbf{R}_{i,j} \end{bmatrix}$. Therefore, an expression for $\delta\mathbf{p}_i|\mathbf{F}_{i,1}$ is obtained by substituting Eq. (8) into Eq. (9).

$$\delta\mathbf{p}_i|\mathbf{F}_{i,1} = \sum_{j=1}^{n_i}\prod_{l=1}^{n_{i,f}} \left(\mathbf{N}_{i,l}\right) \prod_{k=n_{i,f}}^{j+1} adj(\mathbf{S}_{i,k})^{-1}\delta\mathbf{e}_{i,j} \tag{10}$$

The expression of Eq. (10) can be written in the following compact form:

$$\delta\mathbf{p} = \mathbf{M}_i\delta\mathbf{e}_i = \left[\delta\mathbf{p}_r \;\; \delta\mathbf{p}_t\right]^T \tag{11}$$

where $\mathbf{M}_i = \left[\mathbf{M}_{i,1} \ldots \mathbf{M}_{i,ni}\right]$, and $\delta\mathbf{e}_i = \left[\delta\mathbf{e}_{i,1}^T \ldots \delta\mathbf{e}_{i,n_i}^T\right], \mathbf{M}_{i,j} = \prod_{l=1}^{n_{i,f}}(\mathbf{N}_{i,l}) \prod_{k=n_{i,f}}^{j+1} \left(adj(\mathbf{S}_{i,k})^{-1}\right); \delta\mathbf{p}_r$ and $\delta\mathbf{p}_t$ are the orientation and translational errors of the end effector, respectively.

2.2.2 Parallel mechanism

Parallel manipulators are composed of several and identical kinematic chains that connect a fixed basis to a movable platform. Differently of serial manipulators, the parallel manipulators are subject to kinematic constraints introduced by their closed-loop kinematic configurations. These kinematic constraints must be considered to propagate the errors of the joint clearance onto the end effector. Moreover, the pose obtained from any kinematic chain should be equal to each other; therefore, $\mathbf{P}_1 = \mathbf{P}_2 \cdots = \mathbf{P}_m$.

For the model of the joint clearances, the external load that acts on the end effector produces the errors in the joint clearance of the kinematic chains. The errors of the joints are correlated due to the kinematic constraints of the parallel mechanism, as shown in Fig. 2.

The following assumptions are considered:

(1) The errors of all the joint clearances of each kinematic chain defined by $\delta\mathbf{e}_i$ are correlated. This correlation depends on the orientation of the kinematic chains, $\mathbf{R}_i$, concerning the fixed frame. Thus, $\delta\mathbf{e}_i = \mathbf{Q}_i\left[\delta\mathbf{e}_{i,1}^T \ldots \delta\mathbf{e}_{i,n_i}^T\right]$ with $\mathbf{Q}_{i,j} = \begin{bmatrix} \mathbf{R}_i & \mathbf{0}_{3\times3} \\ \mathbf{0}_{3\times3} & \mathbf{R}_i \end{bmatrix}$.

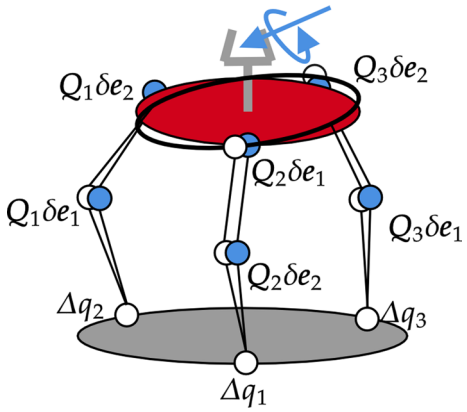

Fig. 2 Model of a parallel mechanism subject to clearances

(2) The passive joints are free. Therefore, no clearance around the axial axis is considered for the passive joints, and thus, $\Delta\beta_{i,j,z} = 0$.
(3) The errors of the prismatic or revolute active joints are entirely independent. They are defined by $\Delta\mathbf{q} = \left[\Delta q_1 \ldots \Delta q_m\right]^T$.

The errors of the joint clearances are propagated for every single kinematic chain by using the expression of Eq. (10), and the error produced by the active joints is also considered by using the Jacobian matrix $\mathbf{J}$.

$$\delta\mathbf{p}_i = \mathbf{W}\mathbf{J}^{-1}\delta\Delta\mathbf{q} + \mathbf{M}_i\delta\mathbf{e}_i \tag{12}$$

where $\mathbf{W}$ transforms the end-effector error to an error screw according to the screw theory [34]. The definition of this matrix will depend on the kinematics of the parallel mechanism. The smaller error along each Cartesian coordinate of the errors of every kinematic chain $\delta\mathbf{p}_i$ is considered in order to respect the kinematic constraints of the parallel mechanism ($\mathbf{P}_1 = \mathbf{P}_2 \cdots = \mathbf{P}_m$). Thus, the total error screw in the end effector of the parallel mechanism $\delta\mathbf{p}$ is defined by the following expression.

$$\delta\mathbf{p} = \min\left(\delta\mathbf{p}_1 \;\; \delta\mathbf{p}_2 \;\; \ldots \;\; \delta\mathbf{p}_m\right) = \left[\delta\mathbf{p}_r \;\; \delta\mathbf{p}_t\right]^T \tag{13}$$

with $\delta\mathbf{p}_r$ and $\delta\mathbf{p}_t$ being the orientation and translational errors, respectively.

3 Definition of the global kinematic reliability criterion

Kinematic reliability is the probability that the mechanism performs a specific motion not exceeding an error limit. These motion errors can be produced by uncertainties in

the geometric parameters and clearances of the manipulator [35].

As presented in the previous section, the uncertain parameters of the joint clearances can be modeled as random variables. These random variables are grouped in the random vector $\mathbf{c}$ of Eq. (4) associated with the joint probability density function $f_{\mathbf{c}}(\mathbf{c})$. The kinematic error or the performance function is defined as $e_T(\mathbf{c})$ based on the error screw definition of Eqs. (11) and (13) for serial and parallel manipulators, respectively. It is worth mentioning that the kinematic error for the performance function, e_T, can consider the orientation error ($e_T(\mathbf{c}) = ||\delta\mathbf{p}_r||$) or the translational error ($e_T(\mathbf{c}) = ||\delta\mathbf{p}_t||$) separately, where ||.|| represents the magnitude of the vector. The kinematic reliability is quantified by the probability of the positioning error, $e_T(\mathbf{c})$, exceeding the maximum admissible limit, e_{max}, and thus,

$$p_f = pr\{e_T(\mathbf{c}) > e_{max}\} \tag{14}$$

where $pr\{.\}$ represents the probability.

Several methods have been used in the literature to evaluate the kinematic reliability as stated in the literature review of the introduction [27–29]. In this contribution, the failure probability is computed by using the Monte Carlo simulation method, the first-order reliability method (FORM), and the second-order reliability method (SORM). These methods are described in Appendix A.

The kinematic reliability according to Eq. (14) is only evaluated in a specific configuration, and therefore, it represents the probability of the kinematic error exceeding the maximum limit only in this particular configuration.

The concept of the global criteria has been used to evaluate kinematic properties of the manipulator such as the global conditioning index (GCI) [4]. Consequently, the global reliability index (GRI) aims at evaluating the behavior of the kinematic reliability over the workspace of the manipulator. Therefore, the following global reliability index is proposed:

$$GRI = \frac{\int_w p_f dw}{\int_w dw} \tag{15}$$

where p_f is the probability that the kinematic error exceeds the maximum limit at a single point of the workspace w; this probability is evaluated by using the expression of Eq. (14). The denominator represents the volume of the workspace. The failure probability, p_f, is bounded as follows:

$$0 \leq p_f \leq 1 \tag{16}$$

that also produces a bounded global performance index defined as:

$$0 \leq GRI \leq 1 \tag{17}$$

where the desired performance of a manipulator consists of minimizing the failure probability and the global reliability index.

The proposed concept of the global reliability index will be applied to three different types of manipulators.

4 Applications

This section presents three examples to illustrate the application of the global reliability. The examples consider a serial 3R manipulator, a 2-DOF planar parallel manipular, and a Cartesian parallel manipulator (CPM).

Initially, the rotational joint clearances used in all the applications are defined. The parameters of the active joint clearances, according to the model of Eq. (3), are defined as $\beta_{xy} = 0.1^o$, $\beta_z = 0.05^o$, $b_{xy} = 5 \times 10^{-5}$m, $b_z = 5 \times 10^{-5}$m, and $\gamma_{i,j} = 180^o$. The passive joints have same parameters; nevertheless, no clearance around the axial axis is considered, and thus, $\beta_z = 0^o$. Then, the performance function is defined according to the expression of Eq. (14). Thus, the positioning error is considered in the analysis, and thus, $e_T(\mathbf{c}) = ||\delta\mathbf{p}_t||$ and $e_{max} = 1 \times 10^{-3}$m. Finally, the following hardware was used: i7 Intel i7-7500U CPU processor (2.9 GHz) and RAM 8.0 GB.

The global conditioning index is a criterion widely used in the literature to assess the kinematic dexterity of manipulators [4]; this index has been also evaluated for all the examples in order to establish a basis to compare the results and behavior of the global reliability index proposed in the present contribution.

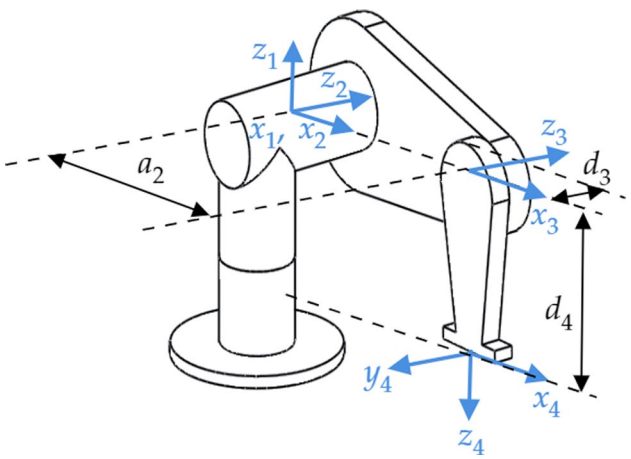

Fig. 3 3R serial manipulator

Table 1 D–H parameters of 3R manipulator

j	α_{j-1}	a_{j-1}	d_j	θ_j
1	0	0	0	θ_1
2	-90^o	0	0	θ_2
3	0	a_2	d_3	θ_3
4	-90^o	0	d_4	0

4.1 3R serial manipulator

The 3R serial arm is presented in Fig. 3, and its D–H parameters are defined in Table 1. According to the error propagation method, $i = 1$ and $j = 1, \ldots, 3$. The link lengths and maximum limits of the rotational joints are defined as $a_2 = 0.15\text{m}$, $d_3 = 0.01\text{m}$, $d_4 = 0.10\text{m}$, $-100^o \leq \theta_1 \leq 90^o$, $-90^o \leq \theta_2 \leq 45^o$ and, $-90^o \leq \theta_3 \leq 90^o$.

Initially, the failure probability of the kinematic reliability is evaluated by using the Monte Carlo simulation (MCS) method, first-order reliability method (FORM) and second-order reliability method (SORM).

The failure probability, p_f, is evaluated at several positions within the workspace as shown in Fig. 4. Figure 4a presents the selected positions over the xz plane considering the y-coordinate fixed at $y = d_3$. Figure 4b presents the positions for the xy plane considering the z-coordinate fixed at $z = 0$.

The outcomes of the failure probability, p_f, are presented in Table 2. Considering the MC as the reference, one can observe that p_f obtained by using SORM and MC is similar in most cases. Nevertheless, the outcomes of p_f obtained by the FORM are different from the MC and SORM outcomes. This indicates that, for this particular application, SORM estimates the failure probability more accurately than FORM since SORM copes properly with the nonlinear kinematic model of the manipulator. Nevertheless, SORM demands higher computational time than MC as presented in Table 2.

One can observe that significant errors were obtained in the estimation of the failure probability by using the SORM regarding the outcomes of the MCS of Table 2, for the points *f*), *g*), *h*), and *i*). According to Appendix A, this issue was originated by the unfitting selection of the error tolerance ϵ to solve the optimization problem of Eq. (21) and the small changes in the coordinates ι to evaluate the partial derivatives of Eq. (23). The selection of these parameters is not evident, and it has a high influence on computation time and accuracy. For this application, the parameters were selected by trial and error to obtain the best outcomes, and thus, $\epsilon = 1 \times 10^{-3}$ and $\iota = 1 \times 10^{-4}$. Nevertheless, it is observed that the SORM estimates the failure probability successfully for most of the cases.

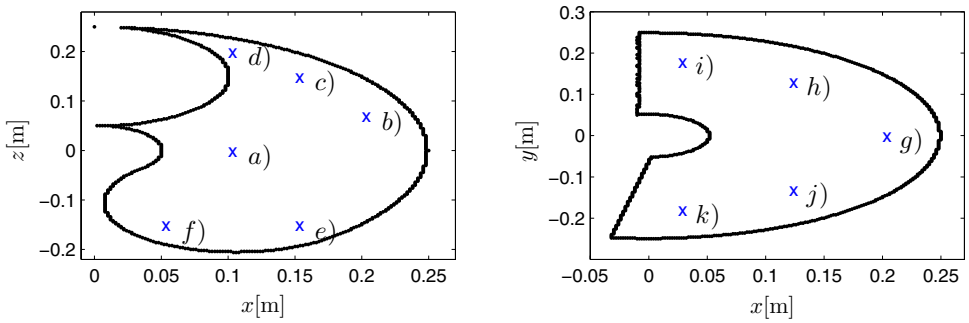

(a) xz plane. **(b)** xy plane.

Fig. 4 Usable workspace of the 3R serial manipulator

Table 2 Parameters and variables

p	p_f(MCS)	p_f(FORM)	p_f(SORM)	Time (MCS) [s]	Time (SORM) [s]
(a)	4.0×10^{-5}	7.4×10^{-5}	3.7×10^{-5}	0.586330	2.569838
(b)	0.0908	0.0451	0.1001	0.518443	1.909145
(c)	0.0664	0.0386	0.0666	0.542946	1.584551
(d)	0.0934	0.0436	0.0935	0.580253	2.421109
(e)	0.0704	0.0203	0.0744	0.546025	1.638136
(f)	0.0014	5.06×10^{-11}	5.83×10^{-11}	0.546202	3.010653
(g)	0.0036	6.3×10^{-4}	8.2699×10^{-4}	0.544293	3.630847
(h)	0.0019	4.9×10^{-4}	0.0011	0.594853	2.102882
(i)	0.0037	1.018×10^{-4}	3.78×10^{-4}	0.583194	3.217070
(j)	0.0020	0.0026	0.0019	0.568650	2.462535
(k)	0.0039	0.0051	0.0021	0.542009	2.580229

The kinematic reliability is also evaluated over the usable workspace as shown in Fig. 5. The p_f increases in the outer limit of the usable workspace that corresponds to poses in which the 3R manipulator is extended. The increment of p_f is produced by increasing the kinematic error in the outer borders of the usable workspace. The left side of the usable workspace corresponds to poses in which the manipulator is retracted; therefore, the kinematic error and p_f decrease (see Fig. 5a, b).

Moreover, the kinematic dexterity based on the condition number of the Jacobian matrix is also computed over the usable workspace as presented in Fig. 6. The local kinematic dexterity corresponds to $1/\kappa(\mathbf{J})$, where $\kappa(.)$ is the condition number of a matrix, and $\mathbf{J}$ is the Jacobian matrix. For this specific application, an inverse relationship between kinematic reliability (see Fig. 5) and kinematic dexterity is observed (see Fig. 6) for the poses in which the manipulator is extended, i.e., p_f increases and $1/\kappa(\mathbf{J})$ decreases. Nevertheless, this behavior is not observed for the poses in which the manipulator is retracted.

The definition of both the probability of failure and the kinematic dexterity is related to positioning error. The augment of the probability of failure p_f implies the increase in the end-effector positioning error, as defined in Eq. (14). The kinematic dexterity depends on the rank of the Jacobian matrix that measures the impact of the joint error on the positioning error of the end effector. Thus, a high kinematic dexterity implies a small effect of the joint errors on the end-effector positioning error. Consequently, an inverse relationship between the

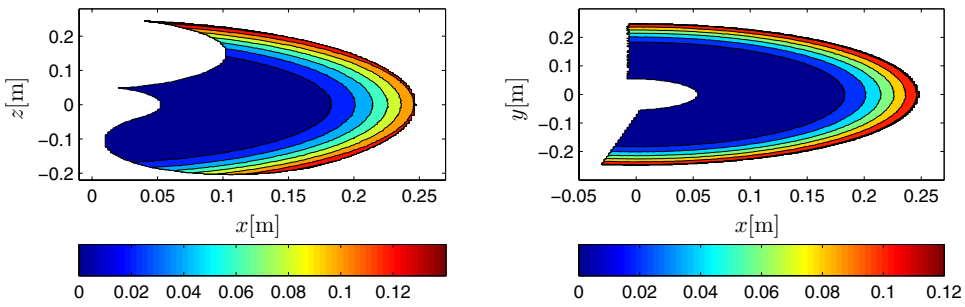

Fig. 5 p_f over the usable workspace

(a) xz plane. **(b)** xy plane.

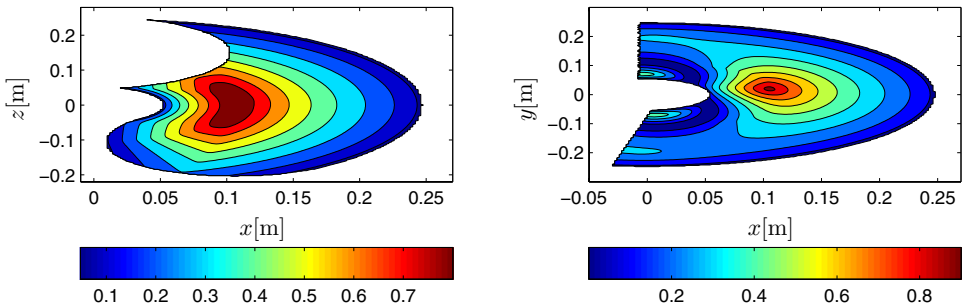

Fig. 6 $1/k(\mathbf{J})$ over the usable workspace

(a) xz plane. **(b)** xy plane.

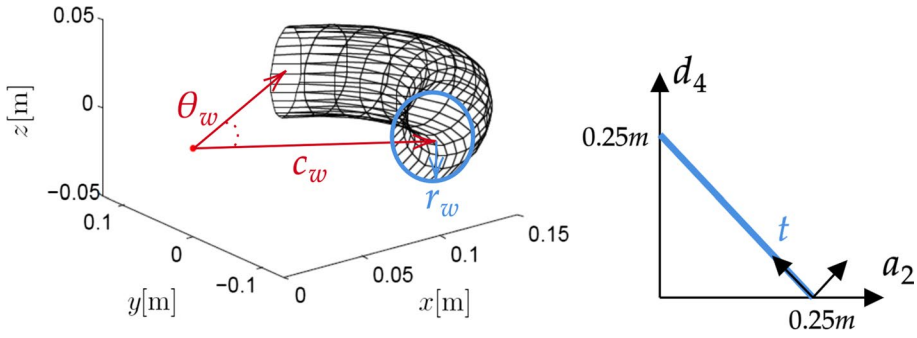

Fig. 7 Dimensional definitions

(a) Torus part workspace. **(b)** t coordinate definition.

probability of failure and the kinematic dexterity is observed for this application.

Finally, the global reliability index (GRI) is also evaluated as follows. The volume of the workspace for the computation of the GRI is defined as a torus part, w (see Fig. 7a). The volume w is inscribed within the usable workspace, and it is defined as a function of the link lengths as follows:

$$w = \pi r_w^2 c_w \theta_w \tag{18}$$

where r_w is the radius of the tube; c_w is the distance of the center of the torus to the center of the tube; θ_w is the angle of the torus part. The geometric parameters of the torus part are defined as a function of the link lengths, and thus, if $a_2 \leq d_4$, then $r_w = d_4/4$, and $c_w = a_2$, and if $a_2 < d_4$, then $r_w = a_2/4$, and $c_w = d_4 + a_2/2$.

For this analysis, the link lengths a_2 and d_4 are considered as variables. Thus, $0 \leq a_2 \leq 0.25$m and $0 \leq d_4 \leq 0.25$m; moreover, the following geometric constraint is imposed:

$$a_2 + d_4 = 0.25\text{m} \tag{19}$$

Based on this geometric constraint, an auxiliary coordinate, t, is defined to evaluate all the possible combinations of the link lengths, and thus, $t = 2/\sqrt{2}a_2$ (see Fig. 7b).

The GRI is assessed for all the combinations of the link lengths subject to the imposed geometric constraint of Eq.(19) based on the definition of the auxiliary coordinate t (see Fig. 8). Moreover, the global conditioning index (GCI) is also computed. One can observe that the behavior of the GRI is inversely proportional to the GCI, i.e., the increase in the global failure probability decreases the global kinematic dexterity. The maximum value of the GRI is 0.02974 for $t = 0.1768$m.

4.2 5R planar parallel mechanism

The 5R symmetrical planar parallel mechanism has two identical kinematic chains designated by $i = 1, 2$. Each kinematic chain has an active, θ_{a_i}, or actuated joint, one passive joint, θ_{p_i}, and two links, L_i, for $i = 1, 2$. The active joints are located at the point A_i. The geometry of the 5R symmetrical parallel mechanism is illustrated in Fig. 9.

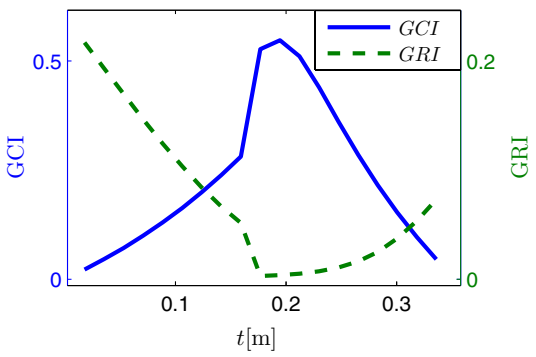

Fig. 8 GCI and GRI of the 3R manipulator

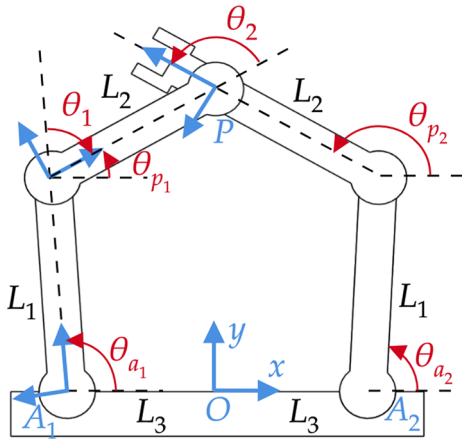

Fig. 9 5R parallel planar manipulator

The end effector of the mechanism is located at the point P joined to the second kinematic chain, and its position is defined by the x and y Cartesian coordinates. Additionally, the fixed reference frame O is defined at the midpoint of A_1A_2, and this length is defined as L_3. The D–H parameters of the second kinematic chain from the frame O to P are presented in Table 3. The link lengths defined for this numerical application are $L_1 = 0.12$m, $L_2 = 0.10$m, and $L_3 = 0.08$m. The orientation of the kinematic chains $\mathbf{Q}_i$ is defined by the orientation matrices: $\mathbf{R}_1 = \mathbb{I}_{3x3}$, and $\mathbf{R}_2 = \mathbb{I}_{3x3}$. According to Eq. (12), the positioning error is evaluated with $\mathbf{W} = [\mathbf{0}\,\mathbb{I}_{3x3}]^T$.

Initially, the usable workspace, maximum inscribed workspace (MIW), and locus singularities are presented in Fig. 10a considering the link's length defined for this numerical application as in [5, 18]. Additional details about the kinematic model of 5R symmetrical parallel robot are presented by Liu et al. [5]. Moreover, the kinematic dexterity based on the inverse conditional number of the Jacobian matrix $k(\mathbf{J})$ is evaluated over the usable workspace (see Fig. 10b). It is observed that the kinematic dexterity decreases close to the singular loci.

The kinematic reliability was estimated using the MC method over the usable workspace (see Fig. 11a). Differently from the serial manipulator, one can observe that the failure probability increases close to type II singular loci positions, i.e., the kinematic error increases by the inversion of

Table 3 D–H parameters of 5R parallel manipulator

j	α_{j-1}	a_{j-1}	d_j	θ_j
1	0	$-L_3$	0	θ_{a_1}
2	0	L_1	0	θ_1
P	0	L_2	0	θ_2

the singular Jacobian matrix according to Eq. (12). Therefore, there is an inverse relationship between the kinematic dexterity and the probability of failure close to type II singularities. The regions of the workspace close to the type II singular loci correspond to configurations in which the Jacobian matrix is ill-conditioned; this condition implies that the effect of the joint error on the positioning error of the end effector is higher than other configurations. It is worth mentioning that the probability of failure and the kinematic dexterity are based on the positioning error. Therefore, the augment of the end-effector positioning error leads to increases in the probability of failure p_f according to Eq. (14).

The kinematic reliability is also computed over the maximum inscribed workspace (*MIW*) (see Fig. 11b). The highest value of p_f is obtained at the bottom side of the *MIW* close to the type II singular loci. The *MIW* is considered to compute the global reliability index (GRI).

Finally, the GRI over the MIW is computed. For this analysis, the link lengths are considered as variables, and thus, $0 \leq L_1 \leq 0.3$m, $0 \leq L_2 \leq 0.3$m, and $0 \leq L_3 \leq 0.15$m. Moreover, the following geometric constraint for the link lengths is considered $L_1 + L_2 + L_3 = 0.3$m to evaluate the combination of all possible combinations of the link lengths. Consequently, Fig. 12a shows the global reliability index evaluation considering the variable link lengths. It can be observed that on the left side of the surface the global reliability is smaller than in other regions, and for this condition, the link lengths correspond to $L_2 > L_1 + L_3$, and the highest global reliability is obtained for $L_3 = 1.5$m. On the other hand, Fig. 12b shows the global conditioning index; it is observed that the highest values of global conditioning

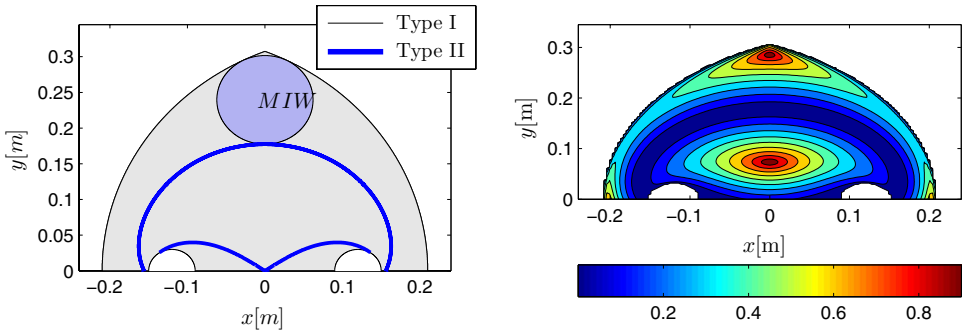

Fig. 10 Usable workspace

(a) Singular loci. **(b)** Local conditioning index.

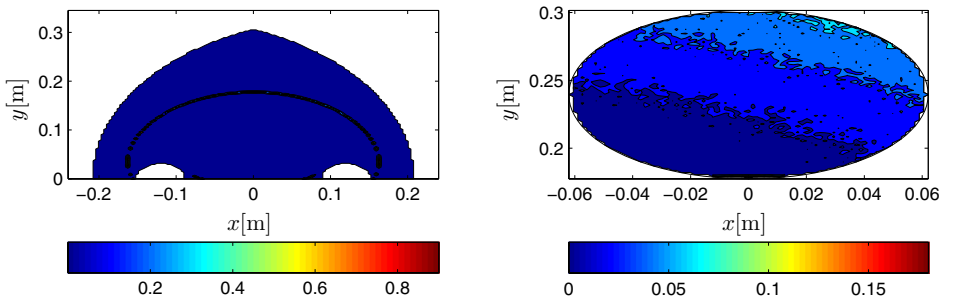

Fig. 11 Failure probability p_f

(a) Usable workspace. **(b)** Maximum Inscrived Workspace (MIW).

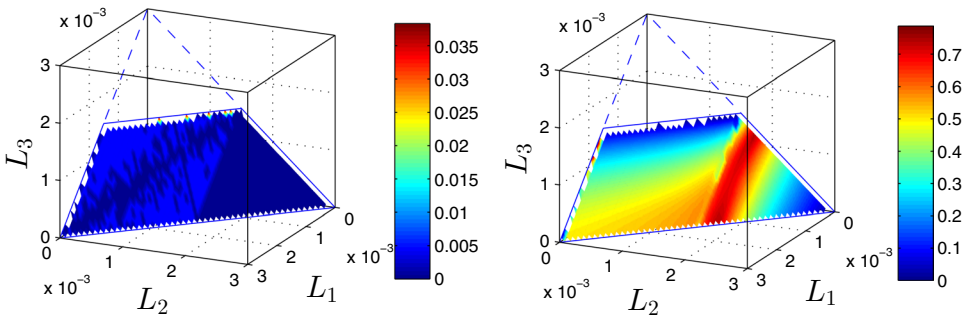

Fig. 12 Length links surface

(a) Global reliability index. **(b)** Global conditioning index.

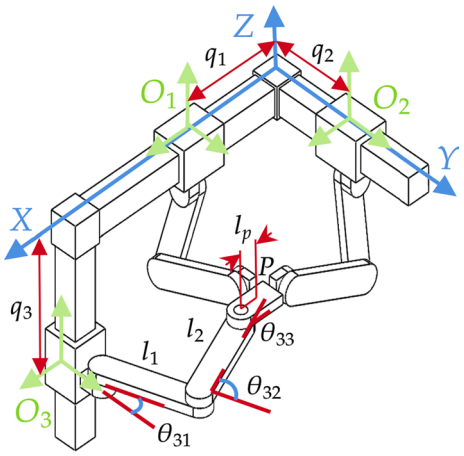

Fig. 13 Cartesian parallel manipulator (CPM)

Table 4 D–H parameters of Cartesian parallel manipulator

j	α_{j-1}	a_{j-1}	d_j	θ_j
1	0	0	0	$\theta_{j,1}$
2	0	l_1	0	$\theta_{j,2}$
3	0	l_2	0	$\theta_{j,3}$
P	0	l_p	0	0

correspond to the lowest results of the global reliability index. Therefore, there is a correlation in the behavior of global reliability index and global conditioning index for this manipulator.

4.3 Cartesian parallel manipulator

The Cartesian parallel manipulator (CPM) is presented in Fig. 13. CPM has three symmetric kinematic chains that joint the moving platform P to the fixed frame. Every kinematic chain is located at the frame O_j, and it has three passive rotational joints defined by passive joint angles $\theta_{j,i}$, for $i = 1, 2, 3$, and $j = 1, 2, 3$. The link lengths of every kinematic chain are defined by l_1, l_2, and l_p defines the length of the moving platform. The three active prismatic joints ($\mathbf{q} = [q_1 \ q_2 \ q_3]^T$) act along the X, Y and Z axes. The moving platform has three translational degrees of freedom defined by the Cartesian axes (x, y, z).

Concerning the kinematic model, the Cartesian position of the moving platform is directly defined by the prismatic active joints, and thus, $q_1 = x$, $q_2 = y$, and $q_3 = z$. Consequently, the Jacobian matrix is a 3x3 identity matrix, $\mathbf{J} = \mathbb{I}_{3x3}$. The D–H parameters of the $j-th$ kinematic chain from the frame O_j to P are presented in Table 4.

The orientation of the kinematic chains $\mathbf{Q}_i$ is defined by the orientation matrices: $\mathbf{R}_1 = \mathbb{I}_{3x3}$, $\mathbf{R}_2 = \mathbf{R}(90^o, X)$, and $\mathbf{R}_3 = \mathbf{R}(90^o, Y)$. According to Eq. (12), the positioning error is evaluated with $\mathbf{W} = [\mathbf{0}\ \mathbb{I}_{3x3}]^T$.

Initially, the kinematic reliability was estimated over the plane xy of the workspace ($z-$ axis is constant $z = 0.08$m) as shown in Fig.14a with the link lengths $l_1 = 0.075$m and $l_2 = 0.075$m and the length of the moving platform $l_p = 0.018$m. This analysis allows examining the local behavior of the kinematic reliability and evaluating the variation of the failure probability at the end effector over the workspace. It is observed that the failure probability increases at the left side of the workspace wherein the third kinematic chain is retracted (see Fig. 14a). Thus, the retraction of the third chain augments the probability of failure.

Finally, the global reliability index is computed as a function of the link lengths by using the auxiliary t coordinate (see Fig. 14b). For this analysis, the link lengths are considered as variables $0.040\text{m} \leq l_1 \leq 0.120\,\text{m}$, $0.040\text{m} \leq l_2 \leq 0.120\text{m}$ and $l_p = \min([l_1 \quad l_2])/8$. Moreover, the following geometric constraint is considered $l_1 + l_2 = 0.15$m. The selected workspace, w, to compute the GRI is considered as a cuboid volume which faces lengths, d_w, are defined as a function of the link lengths, and thus, $d_w = \min([l_1 \quad l_2])/4$, and its centroid is located at the Cartesian coordinate $[d_w/2 \quad d_w/2 \quad d_w/2]$. The t coordinate is stated as $t = 2/\sqrt{2}l_1$ likewise the previous definition of Fig. 7b. The results indicate that the global reliability decreases by increasing the length of the second link l_2, i.e., there is an increase in the failure probability for the cases in which $l_2 > l_1$. Moreover, it is expected that the position accuracy decreases since the global kinematic index augments for configurations in which the second link is larger

Fig. 14 Kinematic reliability

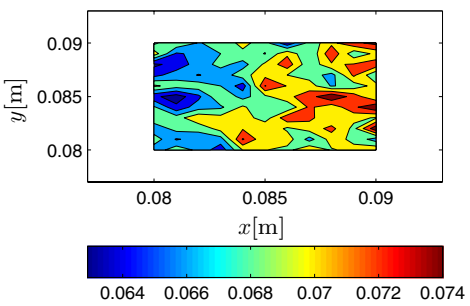

(a) Over the xy plane.

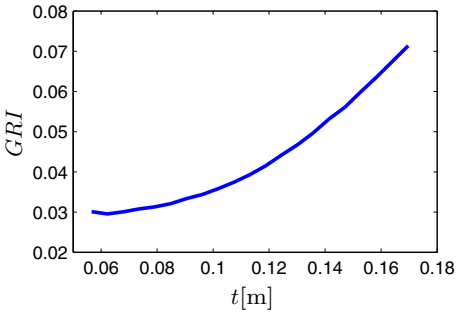

(b) Global reliability index.

than the first one ($l_2 > l_1$). This information could be useful for the selection of the link lengths. In this analysis, the global conditioning index does not exhibit variations since the condition number of the Jacobian matrix is equal to one; therefore, the global conditioning index is not suitable to evaluate the influence of geometric parameters on the kinematic performance error for this particular application.

The global reliability index evaluates the positioning error considering the error of the clearances differently from the global conditioning index that evaluates the kinematic dexterity. However, the global conditioning index indirectly takes into account the measure of positioning accuracy.

5 Conclusions

The global reliability index was evaluated based on the error produced by clearances over a required workspace. Initially, random uncertainties were introduced within the axisymmetric model of the clearances; then, a method to propagate the joint clearances was proposed; finally, the global reliability index was formulated. The proposed approach was applied to serial and parallel manipulators. The numerical results demonstrated that the global reliability index permitted to evaluate the positioning error considering the errors of the joint clearances.

A novel performance criterion applied to robotic manipulators based on kinematic reliability was presented in this contribution. The uncertain error produced by clearances on the kinematic error of the end effector was evaluated over a required workspace by computing the reliability. The uncertainties were introduced in the axisymmetric model of the clearances, and a propagation method to determine the error on the end effector was used to compute the global reliability criterion.

Moreover, the proposed approach allows quantifying the kinematic reliability that takes into account the effect of clearances. The proposed global reliability index was demonstrated to be an alternative design criterion to take into account the effect of clearance in the kinematic accuracy of the manipulators. The kinematic criterion based on the Jacobian matrix does not present the effects of uncertain clearance on the kinematic performance. The global reliability index proposed in this contribution could be used as design criteria in the optimal design of manipulators subjected to uncertainty and clearances.

Future work will encompass the robust optimal design of manipulators based on the proposed reliability method criterion.

Acknowledgements The authors are thankful for the financial support provided by CNPq (Process 427204/2018-6) and CAPES.

A reliability methods

A.1 Monte Carlo simulation method

The MC method is composed of three steps: *i*) the uncertain parameters of the clearances $\mathbf{c}$ (see Eq. 4) are sampled to obtain a set of n_s random inputs; *ii*) the kinematic error $\delta\mathbf{p}(\mathbf{c})$ is computed for each random input; *iii*) the probability of failure is computed as:

$$p_f = \frac{n_f}{n_s} \tag{20}$$

where n_f is the number of samples that exceed e_{max}.

A.2 First-order reliability method (FORM)

This method is used to evaluate the failure probability of Eq. (14). The performance function $\delta\mathbf{p}(\mathbf{c})$ to evaluate the kinematic error is approximated by a first-order Taylor expansion. Initially, the random vector $\mathbf{c}$ is transformed into random normal variables $\mathbf{u}$. Then, $\delta\mathbf{p}(\mathbf{c})$ is linearized at the most probable point (MPP) $\mathbf{u}^*$ and the reliability coefficient β is computed by solving the following optimization problem:

$$\begin{aligned} &\min_{\mathbf{u}} \beta = ||\mathbf{u}^T\mathbf{u}|| \\ &\text{subject to:} \\ &\delta\mathbf{p}(\mathbf{u}) = e_{max} \end{aligned} \tag{21}$$

where ||.|| represents the magnitude of the vector. Finally, the probability of failure p_f is estimated according to the following expression: $p_f = \boldsymbol{\Phi}[-\beta]$, where $\boldsymbol{\Phi}[.]$ represents the standard normal cumulative distribution. The optimization problem to find the reliability coefficient β was solved by using the algorithm proposed by Rackwitz [36]. The numerical implementation of the algorithm demands the definition of an error tolerance, ϵ, to evaluate the convergence of β, and a small change in the coordinates, ι, to numerically evaluate the partial derivatives for the first-order Taylor expansion [36].

A.3 Second-order reliability method (SORM)

Differently from the FORM, this method aims at evaluating the reliability of system which performance functions is nonlinear. The performance function of the present contribution, $\delta\mathbf{p}(\mathbf{c})$, is based on the nonlinear kinematic model of the manipulator. The Taylor series expansion of the nonlinear function $\delta\mathbf{p}(\mathbf{u})$ at the MMP $\mathbf{u}^*$ is defined as:

$$\begin{aligned}\delta\mathbf{p}(\mathbf{u}) =&\delta\mathbf{p}(u_1, u_2 \dots u_{n_j}) = \delta\mathbf{p}(u_1^*, u_2^* \dots u_{n_j}^*) \\ &+ \sum_{j=1}^{n_j} \frac{\partial\delta\mathbf{p}}{\partial u_j}(u_j - u_j^*) \\ &+ \frac{1}{2}\sum_{k=1}^{n_j}\sum_{j=1}^{n_j} \frac{\partial^2\delta\mathbf{p}}{\partial u_k \partial u_j}(u_k - u_k^*)(u_j - u_j^*)\end{aligned} \tag{22}$$

where these derivatives are evaluated at the MMP $\mathbf{u}^*$. SORM ignores the terms higher than the second-order terms. The probability of failure is computed by using the closed-form expression for the probability computation using the theory of asymptotic approximation proposed by Breitung [37], thus:

$$p_f \approx \boldsymbol{\Phi}(-\beta_{FORM}) \prod_{j=1}^{n_j-1}(1 + \beta_{FORM}\kappa_j)^{-1/2} \tag{23}$$

where κ_j represents the principal curvatures of the performance function at the MMP, and β_{FORM} is the reliability coefficient computed by the FORM.

References

1. Lipkin H, Duffy J (1988) Hybrid twist and wrench control for a robotic manipulator. J Mech Trans Autom 110(2):138–144
2. Bowling A, Khatib O (2005) The dynamic capability equations: a new tool for analyzing robotic manipulator performance. IEEE Trans Robot 21(1):115
3. Wang Z, Ji S, Li Y, Wan Y (2010) A unified algorithm to determine the reachable and dexterous workspace of parallel manipulators. Robot Comput Integr Manuf 26(5):454
4. Gosselin C, Angeles J (1991) A global performance index for the kinematic optimization of robotic manipulators. J Mech Design 113(3):220
5. Liu XJ, Wang J, Pritschow G (2006) Performance atlases and optimum design of planar 5R symmetrical parallel mechanisms. Mech Mach Theory 41(2):119
6. Lara-Molina FA, Dumur D, Takano KA (2018) Multi-objective optimal design of flexible-joint parallel robot. Eng Comput 35:2775
7. Siciliano B, Khatib O (2016) Springer handbook of robotics. Springer, Berlin
8. Zhuang H (1997) Self-calibration of parallel mechanisms with a case study on Stewart platforms. IEEE Trans Robot Autom 13(3):387
9. Cetin K, Tatlicioglu E, Zergeroglu E (2019) On operational space tracking control of robotic manipulators with uncertain dynamic and kinematic terms. J Dyn Syst Measure Control 141(1):011001
10. Costa TL, Lara-Molina FA, Junior AAC, Taketa E (2018) Robust H_∞ compu ted torque control for manipulators. IEEE Lat Am Trans 16(2):398
11. Chebbi AH, Affi Z, Romdhane L (2009) Prediction of the pose errors produced by joints clearance for a 3-UPU parallel robot. Mech Mach Theory 44(9):1768
12. Zhu J, Ting KL (2000) Uncertainty analysis of planar and spatial robots with joint clearances. Mech Mach theory 35(9):1239
13. Wang H, Roth B (1989) Position errors due to clearances in journal bearings. J Mecha Trans Autom Design 111(3):315
14. Erkaya S (2012) Position errors due to clearances in journal bearings. Robot Comput Integr Manuf 28(4):449
15. Binaud N, Cardou P, Caro S, Wenger P, et al. (2010) In: ASME 2010 International design engineering technical conferences and computers and information in engineering conference American Society of Mechanical Engineers Digital Collection, pp. 1371–1380
16. Meng J, Zhang D, Li Z (2009) Accuracy analysis of parallel manipulators with joint clearance. J Mech Design 131(1):011013
17. Flores P, Ambrósio J, Claro JP, Lankarani H (2007) Dynamic behaviour of planar rigid multi-body systems including revolute joints with clearance. Proc Inst Mech Eng Part K J Multi-body Dyn 221(2):161
18. Lara-Molina F, Koroishi E, Steffen V, Martins L (2018) Kinematic performance of planar 5R symmetrical parallel mechanism subjected to clearances and uncertainties. J Braz Soc Mech Sci Eng 40(4):189
19. Altuzarra O, Aginaga J, Hernández A, Zabalza I (2011) Workspace analysis of positioning discontinuities due to clearances in parallel manipulators. Mech Mach Theory 46(5):577
20. Venanzi S, Parenti-Castelli V (2005) A new technique for clearance influence analysis in spatial mechanisms. J Mech Design 127(3):446
21. Xu D (2018) Kinematic reliability and sensitivity analysis of the modified delta parallel mechanism. Int J Adv Robot Syst 15(1):1729881418759106
22. Kim J, Song WJ, Kang BS (2010) Stochastic approach to kinematic reliability of open-loop mechanism with dimensional tolerance. Appl Math Model 34(5):1225
23. Pandey MD, Zhang F (2012) System reliability analysis of the robotic manipulator with random joint clearances. Mech Mach Theory 58:137
24. Cui G, Zhang H, Zhang D, Xu F (2015) Analysis of the kinematic accuracy reliability of a 3-DOF parallel robot manipulator. Int J Adv Robot Syst 12(2):15
25. Zhan Z, Zhang X, Jian Z, Zhang H (2018) Error modelling and motion reliability analysis of a planar parallel manipulator with multiple uncertainties. Mech Mach Theory 124:55
26. Zhang D, Han X (2020) Kinematic reliability analysis of robotic manipulator. J Mech Design 142(4):044502
27. Zhang X, Pandey MD, Zhang Y (2014) Computationally efficient reliability analysis of mechanisms based on a multiplicative dimensional reduction method. J Mech Design 136(6):061006
28. Zhang D, Zhang N, Ye N, Fang J, Han X (2020) Hybrid learning algorithm of radial basis function networks for reliability analysis. IEEE Trans Reliab. https://doi.org/10.1109/TR.2020.3001232
29. Wu J, Zhang D, Jiang C, Han X, Li Q (2020) On reliability analysis method through rotational sparse grid nodes. Mech Syst Signal Process 147:107106
30. Wu J, Zhang D, Liu J, Han X (2019) A moment approach to positioning accuracy reliability analysis for industrial robots. IEEE Trans Reliab 69:699
31. Wu J, Zhang D, Liu J, Jia X, Han X (2020) A computational framework of kinematic accuracy reliability analysis for industrial robots. Appl Math Model 82:189
32. Zhang X, Pandey MD (2013) An efficient method for system reliability analysis of planar mechanisms. Proc Inst Mech Eng Part C J Mech Eng Sci 227(2):373

33. Patel S, Sobh T (2015) Manipulator performance measures-a comprehensive literature survey. J Intell Robot Syst 77(3–4):547
34. Gallardo-Alvarado J (2016) Kinematic analysis of parallel manipulators by algebraic screw theory. Springer, Berlin
35. Rao SS, Bhatti P (2001) Probabilistic approach to manipulator kinematics and dynamics. Reliab Eng Syst Saf 72(1):47
36. ComitÉ European de BÉton (CEB), Joint Committee on Structural Safety CEB-CECM-FIP-IABSE-IASS-RILEM (1976) First order reliability concepts for design codes. CEB Bulletin no 112. Comité European de Béton, Paris, France
37. Breitung K (1984) Asymptotic approximations for multinormal integrals. J Eng Mech 110(3):357